Journal of Medicinal Chemistry

ARTICLE

pubs.acs.org/jmc

Targeted Biocompatible Nanoparticles for the Delivery of (−)-Epigallocatechin 3-Gallate to Prostate Cancer Cells

Vanna Sanna,[*,†] Gianfranco Pintus,[*,‡] Anna Maria Roggio,[†] Stefania Punzoni,[‡] Anna Maria Posadino,[†,‡] Alessandro Arca,[§,⊥] Salvatore Marceddu,[∥] Pasquale Bandiera,[‡] Sergio Uzzau,[†,‡] and Mario Sechi[*,§,⊥]

[†]Porto Conte Ricerche, Località Tramariglio, 07041, Alghero, Sassari, Italy

[‡]Department of Biomedical Sciences, Centre of Excellence for Biotechnology Development and Biodiversity Research, University of Sassari, Sassari, Italy

[§]Dipartimento Farmaco Chimico Tossicologico, Università di Sassari, 07100 Sassari, Italy

[∥]Istituto di Scienze delle Produzioni Alimentari (ISPA), CNR, Sezione di Sassari, Italy

ABSTRACT: Molecular targeted cancer therapy mediated by nanoparticles (NPs) is a promising strategy to overcome the lack of specificity of conventional chemotherapeutic agents. In this context, the prostate-specific membrane antigen (PSMA) has demonstrated a powerful potential for the management of prostate cancer (PCa). Cancer chemoprevention by phytochemicals is emerging as a suitable approach for the treatment of early carcinogenic processes. Since (−)-epigallocatechin 3-gallate (EGCG) has shown potent chemopreventive efficacy for PCa, we designed and developed novel targeted NPs in order to selectively deliver EGCG to cancer cells. Herein, to explore the recent concept of "nanochemoprevention", we present a study on EGCG-loaded NPs consisting of biocompatible polymers, functionalized with small molecules targeting PSMA, that exhibited a selective in vitro efficacy against PSMA-expressing PCa cells. This approach could be beneficial for high risk patients and would fulfill a significant therapeutic need, thus opening new perspectives for novel and effective treatment for PCa.

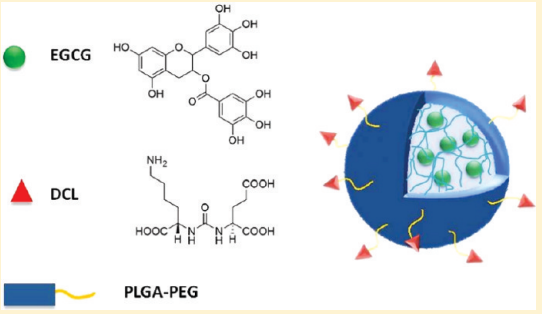

INTRODUCTION

Drug-encapsulated nanoparticles (NPs) have the potential to improve current cancer chemotherapies by increasing drug efficacy, lowering drug toxicity, and maintaining a relatively high concentration of drug at the site of interest.[1−6] This is owed to more specific targeting to tumor tissues via improved pharmacokinetics and pharmacodynamics and active intracellular uptake.[1,7,8] These properties depend on the size and surface characteristics of NPs, as well as on the presence of targeting ligands, which enable NPs to bind to cell-surface receptors and enter cells by receptor-mediated endocytosis.[9,10] Ultimately, active targeting via the inclusion of a specific ligand on the NPs is envisioned to provide the most effective therapy, and some ligand-targeted nanotherapeutics are either approved or under clinical evaluation.[4] As far as the biological targets are concerned, tumor-associated antigens appeared to be suitable biological targets for therapeutic intervention.[11,12] To this end, functionalization of NPs with ligands that bind the extracellular domain of these receptors to selectively target drugs to diseased cells can represent a powerful therapeutic strategy. For example, prostate-specific membrane antigen (PSMA), a well-known transmembrane protein that is overexpressed on prostate cancer (PCa) epithelial cells,[13] has demonstrated a promising potential for PCa therapy.[12,14−16] Recently, in a pioneering work, Farokhzad and Langer developed proof of concept drug delivery vehicles that were composed of biocompatible polymeric [poly(D,L-lactic-*co*-glycolic acid)-*block*-poly(ethylene glycol), PLGA-PEG)] NPs and aptamers to target PSMA and validated them by in vitro and in vivo studies for targeted delivery of docetaxel and uptake by PCa cells.[17,18] The translation of these bioconjugates into clinical practice is expected soon, even though there is continuing interest in developing a localized therapeutic option for treatment of early stage PCa that have reduced toxicity. Thus, prevention and/or chemoprevention, possibly through the use of naturally occurring substances, such as dietary nontoxic phytochemicals, may be the best approach to fight this frequent diseases.[19−21]

On the other hand, green tea, a popular beverage consumed worldwide, has been known to have protective effects against some common types of cancers,[22−26] and green tea catechins (GTCs), expecially (−)-epigallocatechin 3-gallate (EGCG, Figure 1), have been shown to be potent chemopreventive agents in vitro and in many in vivo animal models of induced carcinogenesis.[23,24,27] More recently, clinical trial reports suggested that oral administration of GTCs might be beneficial in

Received: October 21, 2010
Published: February 09, 2011

dx.doi.org/10.1021/jm1013715 | *J. Med. Chem.* 2011, 54, 1321–1332

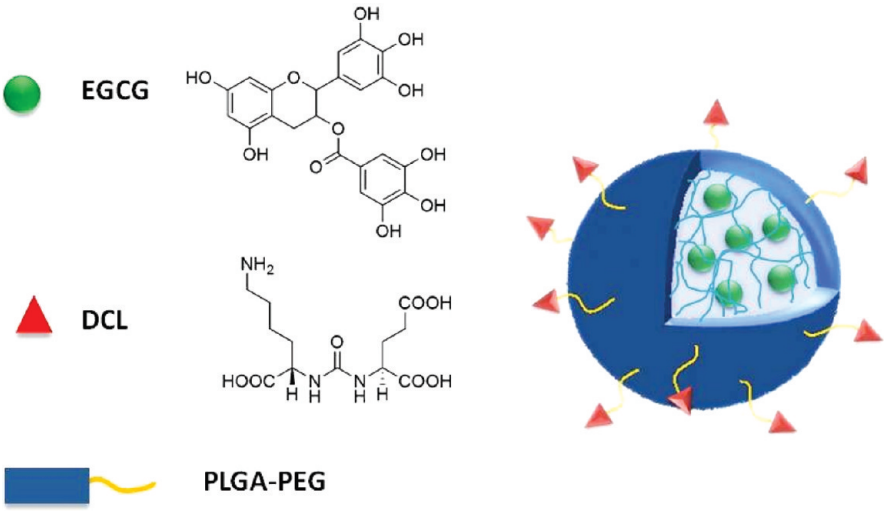

Figure 1. Chemical structure of (−)-epigallocatechin 3-gallate, the anti-PSMA ligand (DCL), and schematic representation of the designed targeted NPs.

the early stage of PCa (on HG-PIN, the main premalignant lesion of PCa), thus preventing almost definitively the cell transformation, leading to a long-lasting inhibition of cancer progression.[28,29] On this basis, because of inefficient or difficult systemic delivery and bioavailability of these promising chemopreventive agents, an improvement of their pharmacological profile using a cell-specific targeting approach is a major challenge, and nanotechnology can represent a powerful strategy.[30] In spite of this, very recently Siddiqui et al. introduced the concept of "nanochemoprevention" which uses nanotechnology for enhancing the outcome of chemopreventive intervention.[20,21] This new approach was used for the first time in 2009 to determine the efficacy of EGCG encapsulated in a polylactic acid−polyethylene glycol (PLA-PEG) NPs in preclinical setting.[27]

In this scenario, by focusing on PCa as a target disease and combining the above-mentioned insights, in particular on recent advances in targeting approaches, we aimed to develop novel targeted EGCG-NPs to be used as nanochemopreventive agents against early stage PCa. According to the following rationale, we report on the design and the development of novel EGCG-encapsulated biocompatible NPs, densely decorated by low-molecular weight organic molecules as targeting ligands in their polymeric shell surface, to selectively bind to PSMA. The goals of the present studies are the following: (1) to develop novel and original polymeric EGCG-encapsulated NPs targeted with small anticancer molecular entities and (2) to evaluate their antiproliferative efficacy with respect to the nontargeted ones.

We chose PLGA-PEG(-COOH) as a polymer system because of its well-established safety profile in clinical use and by considering its biocompatible properties.[6,10,31−33] Moreover, as a further extension of another published study,[34] we selected the pseudomimetic dipeptide *N*-[*N*-[(*S*)-1,3-dicarboxypropyl]carbamoyl]-(*S*)-lysine (DCL, Figure 1) [IUPAC name: 2-{[(5-amino-1-carboxypentyl)carbamoyl]amino}pentanedioic acid] as the PSMA targeting ligand, previously reported by Pomper et al.,[35,36] from a series of urea-based PSMA-inhibitors,[36,37] capable of targeting PSMA with a similar high affinity and specificity to antibodies and aptamers. In this work, the synthetic route to obtain DCL has been revisited and detailed. We therefore synthesized the copolymer PLGA-PEG-DCL, on which PEGylation is considered not only to preserve the antibiofouling properties of NPs but also as a spacer in order to maintain optimal distance between the ligand and the NP surface (see below). To obtain a better control of DCL functionalization, we strategically envisioned preconjugating DCL to the polymer system before nanoformulation. Subsequently, by use of this pseudo-tri-block-copolymer and the parent PLGA-PEG(-COOH), a set of <100 nm targeted (and nontargeted) EGCG-loaded NPs were obtained (Figure 1), which were first submitted to drug-content and drug-release characterization and then evaluated for their ability to selectively inhibit the growth of PSMA positive PCa (LNCaP) cells.

RESULTS AND DISCUSSION

Design of Targeted NPs and Recognition on PSMA Active Site. PSMA (also termed as NAALADase or glutamate carboxypeptidase II) is highly expressed in PCa cells and in nonprostatic tumor neovasculature, and it is currently suitable as a target for anticancer imaging and therapeutic agents.[36,37] Recently, a 3.5 Å solved crystal structure of the PSMA ectodomain[38,39] and several other high-resolution X-ray crystal structures of PSMA with glutamate-containing PSMA inhibitors have been reported.[40] Structural studies established that the PSMA binding site contains two zinc ions located on the amino acid catalytic site. Moreover, a funnel-shaped tunnel with a depth of approximately 20 Å and a width of about 9 Å, near a narrow cavity, is located in proximity of this amino acid binding pocket.[38−41]

In the current study, we sought to synthesize a new polymer by conjugating PLGA-PEG-COOH with a glutamate-containing urea-based inhibitor. We selected an inhibitor containing lysine (DCL, Figure 1), as it contains a primary amine that allows for amide bond formation with carboxyl terminal groups of PEG monomer and also for its high affinity for PSMA (IC_{50s} = 498, from competitive binding assays).[35] To enable high-affinity binding of DCL to PSMA, a methylene chain as spacer (>20 Å) to connect the inhibitor to the NP surface should be envisioned. On this basis, part of the linker portion of PEG would remain outside the tunnel as long as the glutamate moiety is anchored within the binding pocket. Accordingly, we designed a model of conjugated compound PEG-DCL with a linker length of >20 Å.

To investigate the impact of DCL-PEGylation on ligand binding, a comparative docking study was performed. First, free DCL was docked to the PSMA active site, and crucial protein−ligand

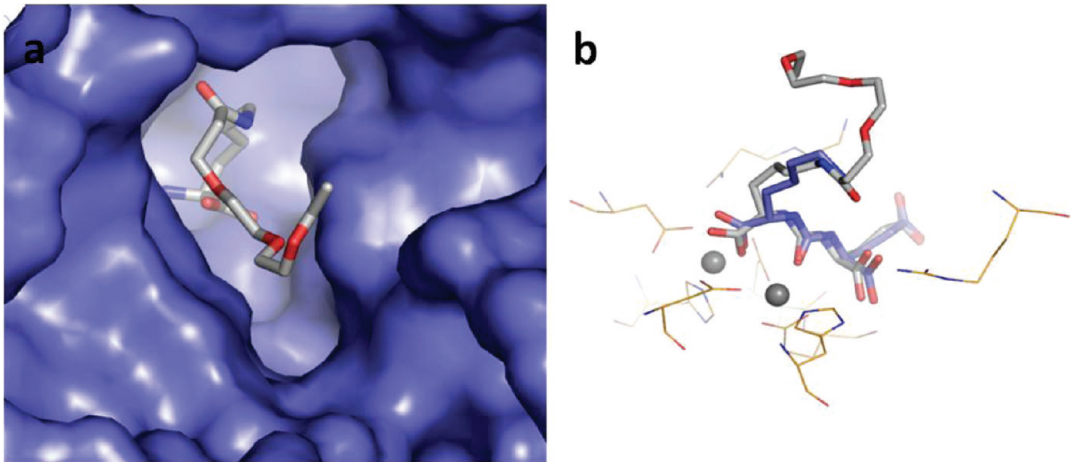

Figure 2. (a) PEG-DCL located in the PSMA tunnel. (b) Docked binding modes of both PEG-DCL and DCL superimposed within the PSMA active site.

interactions were analyzed. In the next step, PEG-DCL was docked and the binding modes of DCL/PEG-DCL were compared. GOLD, version 4.0, was employed to dock DCL and PEG-DCL to PSMA (PDB code 2C6C; for details see Experimental Section). Analysis of the docking results shows that both DCL and PEG-DCL show a good mutual match within the active site. PEG-DCL places its polyether within the tunnel leading from the deeply buried active site to the surface of the PSMA protein (Figure 2a). Both ligands show a consistent binding mode with respect to the DCL moiety: the active site metal ions are well coordinated by the urea oxygen and a carboxylate group (Figure 2b). Favorable interactions are observed between the γ-carboxylate group and Arg210 as well as between urea N−H and C═O of Gly518. The GOLDscore for the DCL binding mode was 86.95. For PEG-DCL it was higher (113.53), as expected because of additional interactions by the PEG chain. To sum up, the comparative docking study showed that introduction of a PEG linker chain most probably has no significant impact on DCL binding to PSMA. Therefore, DCL conjugate polymer seems to maintain good affinity for PSMA, and PEGylated inhibitor can be consequently introduced onto the NP surface.

Synthesis of Di-Block-Copolymer PLGA-PEG-COOH. NPs should ideally have a hydrophilic surface in order to have a minimal self−self and self−nonself interaction, to prevent nanoparticle loss to undesired location, and to escape macrophage capture, enabling "stealth" properties for immune evasion.[42,43] In this way, PEG is widely used for this purpose, and the preparation of PEGylated NPs has been previously investigated and obtained by several synthetic strategies.[10,31−33] One of these involves the availability of the starting polymer (for example, PLGA-PEG), which can be conveniently synthesized by conjugation or polymerization of PEG to PLGA.[10,17,44]

Thus, the starting carboxylate-functionalized di-block-copolymer PLGA-PEG-COOH (Scheme 2; see below) was prepared by conjugating heterofunctional PEG, NH_2-PEG-COOH to PLGA-COOH using standard carbodiimide/NHS-mediated chemistry similar to that reported by Farokhzad et al.,[10,18,44] following a modified procedure. PLGA-COOH was reacted with EDC and NHS in an organic solvent at room temperature to activate the carboxylic acids to the semistable amine-reactive activated NHS-ester of PLGA (PLGA-NHS). The structure of copolymer was confirmed by ^{1}H NMR spectroscopy. Interestingly, a large peak centered at 3.65 ppm, corresponding to the PEG methylene protons, was detected. In fact, analysis of proton intensities, used for determination of the composition of the copolymers, revealed an increased efficacy of PEG conjugation to PLGA (PLGA/PEG approximately in 1:1.5 molar ratio), as previously described.[33] We confirmed that the optimal combination of parameters resulted when the final coupling reaction was carried out using $CHCl_3$ as a solvent and when the mixture was stirred for 24 h.

Synthesis of Targeting Ligand DCL. In addition to its remarkable affinity to PSMA, this small organic molecule was considered for its chemical stability and the relative low cost of production, especially when produced in scaled-up quantities. The overall synthetic route for the preparation of DCL is depicted in Scheme 1. In this work, we planned to obtain DCL from the urea-based intermediate **7**, previoulsy reported by Pomper's group.[45] Accordingly, we revisited the preparation of this key intermediate. **7** was synthesized by coupling of bis-4-methoxybenzyl-L-glutamate hydrochloride (**6**) with triphosgene and TEA at 0 °C, followed by the addition of 2-amino-6-*tert*-butoxycarbonyl-aminohexanoic acid 4-methoxybenzyl ester (**3**). Both synthones **3** and **6** were prepared following previously described procedures.[45,46]

Commercially available *N*ε-Boc-*N*α-Fmoc-L-lysine **1** was reacted with 4-methoxybenzyl chloride and cesium carbonate in *N*,*N*-dimethylformamide (DMF) to give the full protected compound **2**. Removal of the Fmoc group using 20% piperidine in DMF provided the desired synthone **3** in good yield. Syntone **6** was synthesized by reacting the bis-glutamic acid (**4**) with PMBC via condensation with ethyl acetoacetate in dry DMF in the presence of *N*,*N*,*N*′,*N*′-tetramethylguanidine. Purification by basic extractions gave protected amino acid **5**, which was then converted to chlorhydrate after treatment with ether hydrogen chloride solution. It is worth noting that when the amount of TEA was increased (molar ratio from 1:1:4 to 1:1:10 for **6**, **3**, and TEA, respectively), repeating the previoulsy described reaction conditions,[45] pseudo-dimeric urea **8** was obtained (Scheme 1, method A). We found better results when free amine **3** in TEA solution was added to hydrochloride derivative **6** (Scheme 1, method B). For the final step reaction, both the *tert*-butyloxycarbonyl (Boc) and the *p*-methoxybenzyl (PMB) groups of **3** were conveniently removed at room temperature by using

Scheme 1. Synthetic Route for the Preparation of DCL[a]

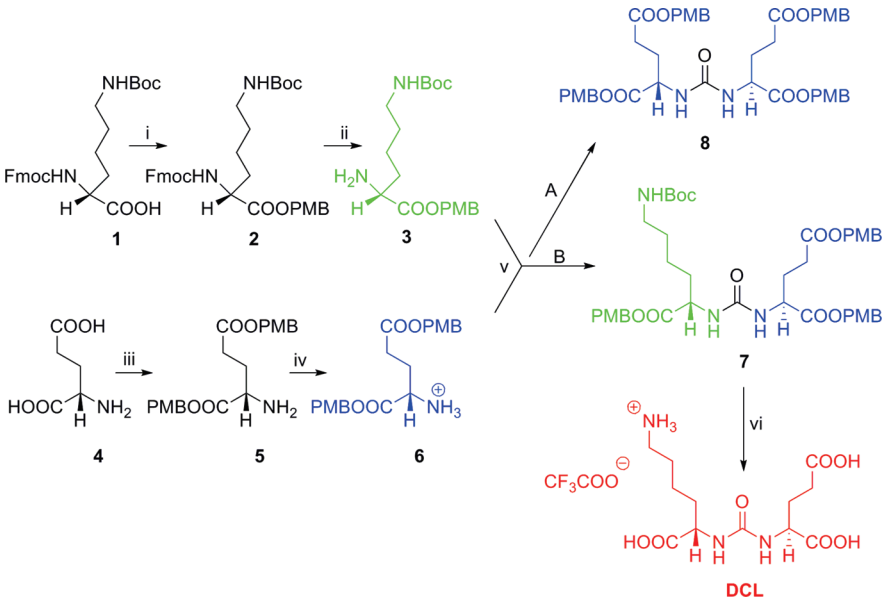

[a] Reagents and conditions: (i) Cs_2CO_3, PMBC, DMF, N_2, room temp for 4 h; (ii) 20% soln of piperidine in DMF, room temp for 2 h; (iii) *N,N,N′,N′*-tetramethylguanidine, DMF, 0 °C, 30 min, ethyl acetoacetate, room temp for 2 h, PMBC, room temp for 24 h; (iv) 4 M HCl in diethyl ether, acetone; (v) (A) triphosgene, **3**, TEA, 10 equiv, CH_2Cl_2, N_2, −78 °C for 1 h, then 30 min at room temp, →**6**, room temp for 12 h; (B) triphosgene, **6**, TEA, 2 equiv, CH_2Cl_2, N_2, 0 °C for 15 min, →**3**, TEA, 2 equiv, room temp for 2 h; (vi) TFA, CH_2Cl_2, room temp for 2 h.

trifluoroacetic acid (TFA)/CH_2Cl_2 solution, to achieve the desired ligand DCL in moderate/good yields. A full characterization of DCL and intermediates was assessed by means of NMR, MS, and elemental analyses.

Synthesis of Pseudo-Tri-Block-Copolymer PLGA-PEG-DCL. The strategy of the block copolymers as preconjugated starting material has been previously proposed for targeted NPs-aptamer bioconjugated for cancer therapy.[17,18] This synthetic approach results in precisely engineered NPs, reducing the batch-to-batch variations in their biophysicochemical properties.

In this way, we developed a prefunctionalized biopolymer, PLGA-PEG-DCL, that has all of the desired NPs components to avoid the postparticle modifications. Conjugation of targeting agent DCL to functional PEG termini was performed with the use of electrophilic NHS esters of PEG carboxylic acids. Reaction between the terminal amine group of DCL and PEG-NHS resulted in the formation of physiologically stable amide bonds. The designed PLGA-PEG-DCL copolymer was therefore synthesized by using a two-step reaction, already described for the preparation of the di-block-copolymer. The carboxyl-capped PLGA-PEG-COOH was conjugated to the amine functional group of the DCL, via activation with NHS, to form the intermediate PLGA-PEG-NHS, leading to PLGA-PEG-DCL as a pseudo-tri-block-copolymer (Scheme 2, stage 1). The progress of reaction was monitored by HPLC. For conjugation, increased equivalent ratio of PLGA-PEG-NHS and DCL (from 1:2 to 1:4) improved the conjugation efficiency.

As far as the characterization by ^{1}H NMR is concerned, the resonance shifts of the characteristic PLGA-PEG backbone were detected (steps a−d Scheme 2, stage 1, and Figure 3A). Overlapping signals revealed at 1.56 ppm are attributed to the lactide methyl repeat units. The multiplets at 5.23 and 4.78 ppm correspond to the lactide methine (CH) and the glycolide protons (CH_2), respectively, with a high complexity of peaks resulting from different D-lactic, L-lactic, glycolic acid sequences in the polymer backbone. ^{1}H NMR spectra recorded for PLGA-PEG-DCL also exhibited a series of partially overlapped multiple peaks attributable to the pattern signals of DCL (Figure 3A). Moreover, strong absorption bands in both 225 and 270 nm regions, depicted in UV scan chromatogram (Figure 3B), support the successful conjugation of DCL to PLGA-PEG copolymer.

Nanoformulation and Characterization of Nontargeted and Targeted NPs. Previously, PEGylated urea-based PSMA inhibitor incorporated into a PLA-PEG-PLA derived NPs have been developed.[34] In this work, we used PLGA-PEG-COOH and PLGA-PEG-DCL polymer systems to generate nontargeted and targeted NPs, respectively, as a novel construct. We also planned to obtain NPs of 100 nm lower diameter because of their potential accessibility to and within many disseminated tumors when dosed into a circulatory system, as previously discussed.[4,9]

EGCG encapsulated NPs were prepared using a modified nanoprecipitation method.[44] By precipitation of the PLGA-PEG-COOH and PLGA-PEG-DCL in water, the polymer self-assembles to form polymeric NPs, in which the hydrophobic PLGA blocks form a core to minimize their exposure to aqueous surroundings, whereas the hydrophilic PEG-COOH and PEG-DCL, as flexible moieties, extend from a shell generated to stabilize the core. In particular, the hydrophilic DCL blocks are thrust in aqueous solution onto the NP surface as targeting moieties (Figure 1, Scheme 2, stage 2).

NPs derived from both polymer systems were characterized for their size and surface morphology with SEM (representative images were shown in Figure 4). Particles were characterized by a smooth surface and spherical shape with a narrow size distribution and showed a similar mean diameter (77.18 ± 16.3 nm for NP-1 and 80.53 ± 15.0 nm for NP-2, respectively, Table 1).

As for the drug loading, the amount of EGCG encapsulated in NP-1 resulted in 3.09 ± 0.43 μg/mg, whereas NP-2 was

Scheme 2. Synthesis of Copolymer PLGA-PEG-DCL (Stage 1) and Nanoformulation (Stage 2)[a]

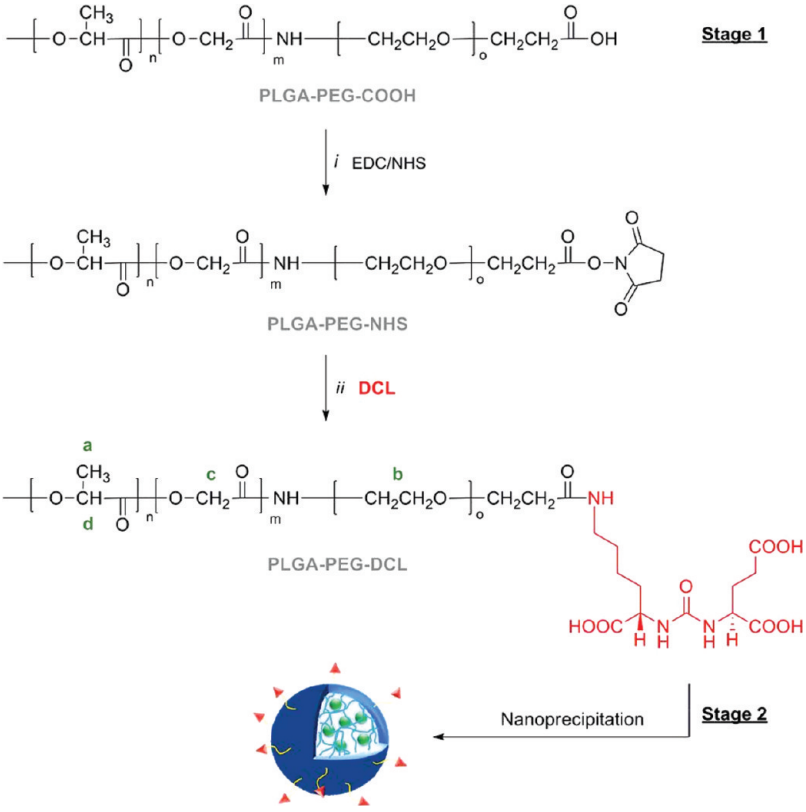

[a] Reagents and conditions: (i) NHS, CH_2Cl_2, EDC, N_2, room temp for 12 h; (ii) DMF, DCL salt, DIPEA, N_2, room temp for 24 h.

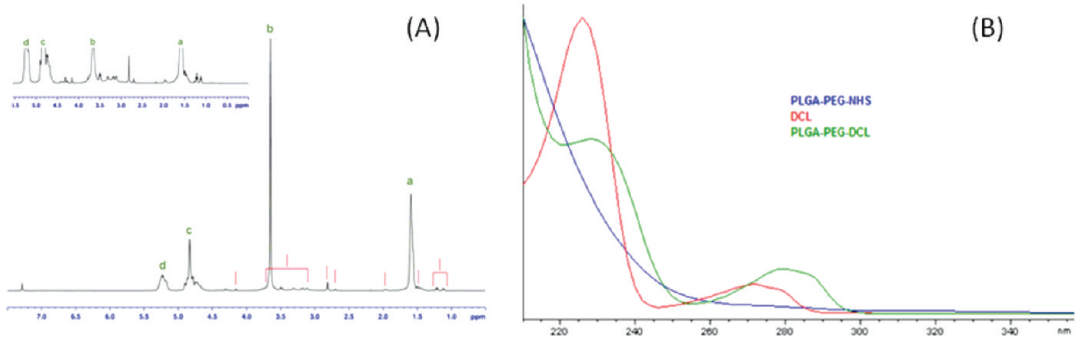

Figure 3. Characterization of PLGA-PEG-DCL: (A) ^{1}H NMR with pattern signals of PLGA-PEG fragment (a−d) and of DCL (red lines); (B) UV spectra comparison of PLGA-PEG-NHS (blue line), DCL (red line), and PLGA-PEG-DCL (green line).

4.81 ± 0.37 μg/mg. Statistical analysis showed that the amount of EGCG encapsulated was significantly larger ($p < 0.05$) for NP-2 with respect to NP-1 (Table 1). It can be ascribed to the higher hydrophilicity of the DCL conjugated polymer (of NP-2) than that of NP-1. Furthermore, the low encapsulation efficiency for both type of NPs (6.18 ± 0.9% and 9.61 ± 0.7% for NP-1 and NP-2, respectively) may be related to the high solubility of EGCG in water, resulting in a significant loss of EGCG instead of being encapsulated by PLGA-PEG blocks. However, interesting yields of production were obtained for both preparations (in the range of 61.50 ± 9.8% and 44.10 ± 1.6% for NP-1 and NP-2, respectively) over multiple experiments.

In Vitro Kinetics Release of EGCG from NPs. The in vitro EGCG release profiles from NPs-1 and NPs-2, compared to the dissolution behavior of pure EGCG, are depicted in Figure 5. The experiments were performed in water (at pH 6.4) and in phosphate buffer solution (PBS) at pH 6.7 and 7.4, chosen to simulate both the slightly acidic microenvironment of extracellular fluid in most tumors and the physiological conditions in normal tissues, respectively.[47] Results show that EGCG alone dissolves very quickly, being highly soluble in water. Conversely, the encapsulation into NPs determined a certain control of EGCG rate release in water, even if about 100% of released EGCG was reached within 2.5 h. Moreover, when both systems (NPs-1 and NPs-2) were tested under the above-mentioned experimental conditions (i.e., PBS, pH 6.7 and 7.4), a similar behavior, confirmed by the overlapping of their kinetics release profiles, was observed. These results can be expected considering

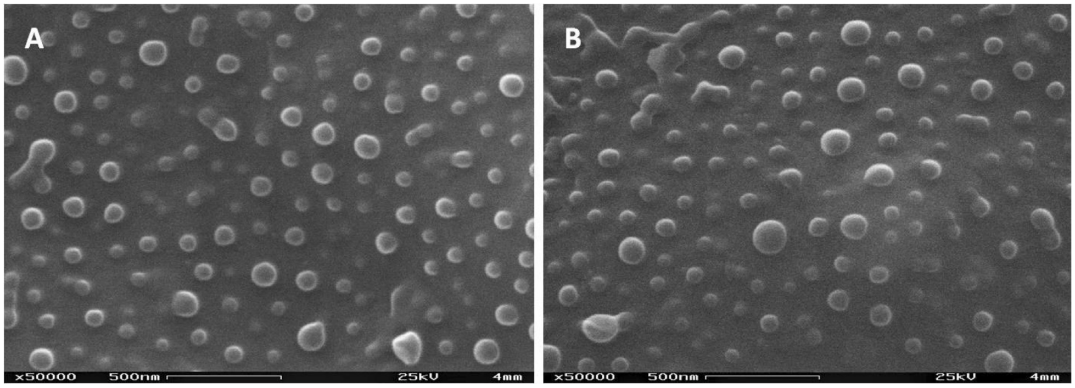

Figure 4. SEM images of nontargeted (NPs-1, A) and targeted (NPs-2, B) EGGC-loaded NPs.

Table 1. Average Diameter, EGCG Content, Encapsulation Efficiency, and Yield of Production of EGCG-Loaded NPs[a]

formulation	average diameter (nm)	EGCG loading (μg/mg)	encapsulation efficiency (%)	yield of production (%)
NP-1	77.18 ± 16.3	3.09 ± 0.43*	6.18 ± 0.9*	61.50 ± 9.8*
NP-2	80.53 ± 15.0	4.81 ± 0.37*	9.61 ± 0.7*	44.10 ± 1.6*

[a] Values presented are the mean ± SD of three preparations. (*) Significant difference ($p < 0.05$).

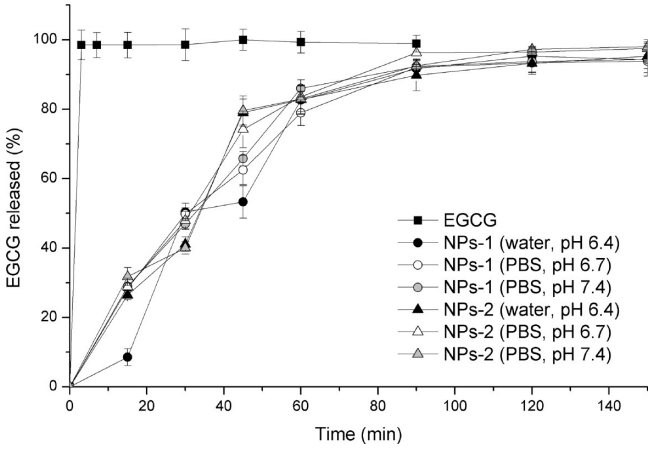

Figure 5. In vitro release profiles of EGCG from NPs (NPs-1 and NPs-2), detected at different pH values and conditions, in comparison with the dissolution rate of the EGCG alone.

the physicochemical properties of the chosen polymers and of EGCG.

The release profiles were obtained by the determination of the EGCG residual amount in NPs during the release experiment (see Experimental Section). To date, only a few studies based on the direct determination of EGCG (and of catechins), released from different types of NPs in the release medium, were reported.[48,49] Similarly, when release studies were performed according to these experiments, a steady-state concentration of EGCG in solution was reached almost immediately, followed by a decrease of EGCG concentration. This apparent loss of EGCG indicates a slow system relaxation to a new equilibrium and was hypothesized to be due to the adsorption of the NPs on the vial walls or attributed to covalent binding of EGCG (or catechins) to the polymer.[48,49] In particular, after re-collection and redispersion of NPs in water, additional EGCG is released and new concentration equilibrium is reached. Following this approach, almost 100% of EGCG was released after three such stages.

This behavior, where nonspecific putative interactions between polymer systems (such as PLGA-PEG-COOH) and EGCG were hypothesized, was further confirmed in this study. In fact, a similar loss of EGCG in solution was observed after exposure of PLGA-PEG-COOH-based unloaded NPs with EGCG free. As displayed in Figure 6, the observed decrease of the band at 275 nm (for EGCG, blue line → black line) and an increase of band in the same absorption range (for PLGA-PEG-COOH-based NPs, green line → red line) suggest a possible EGCG−polymer nanoparticle interaction by a minimal covalent or noncovalent binding of EGCG with the polymer matrix. In summary, it seems that our indirect method enables detection of EGCG by overcoming possible interaction between EGCG−polymer systems.

In Vitro Cellular Cytotoxicity Assays. In order to investigate whether functionalization of NPs with the PSMA inhibitor DCL enhanced the effectiveness of EGCG toward PSMA positive (LNCaP) cells, chosen as a model of PCa tumor lines, we compared the antiproliferative activities of the targeted EGCG-loaded NPs (NPs-2) with those of the nontargeted NPs (NPs-1) in in vitro assays.

LNCaP were exposed to equimolar amounts of EGCG loaded NPs, and two series of experiments were planned and performed (Figure 7). To reduce the effects of nonspecific endocytosis, cells were first exposed to NPs samples for 1 or 3 h and then washed and incubated in NP free medium for 48 and 72 h. To evaluate cytotoxicity, cell counts were conducted directly on LNCaP cells and antiproliferative efficacy was calculated.

After 48 h of incubation, the growth of cells was similar to that of the control for NPs-1 treated for 1 h while cell growth was inhibited for 80% by targeted NPs (NPs-2, Figure 7A). On the other hand, different behavior was found according to the experiment conducted after a 3 h sample exposure. With about 50% and 65% growth inhibition for NPs-1 and NPs-2, respectively, significant antiproliferative activities were detected for both samples. These results clearly demonstrated that targeted NPs were more effective than the nontargeted ones in both assay conditions. Probably when cells were pulsed for only 1 h with

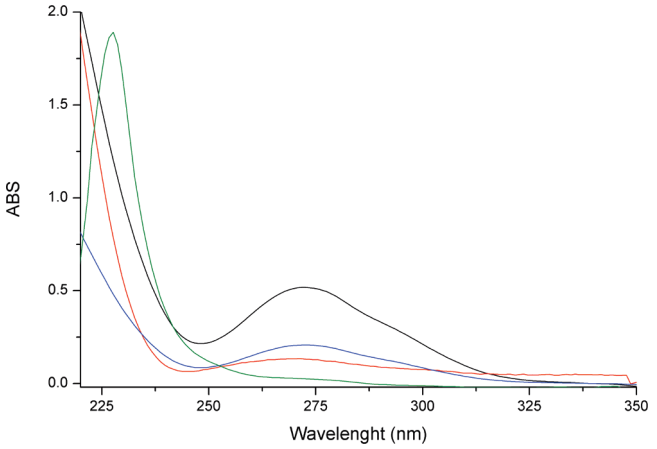

Figure 6. UV measurements of interaction between PLGA-PEG-COOH-based unloaded NPs (green line) and EGCG (black line). Putative polymer−EGCG interaction is depicted by a red line, while the decrease of EGCG is indicated by a blue line.

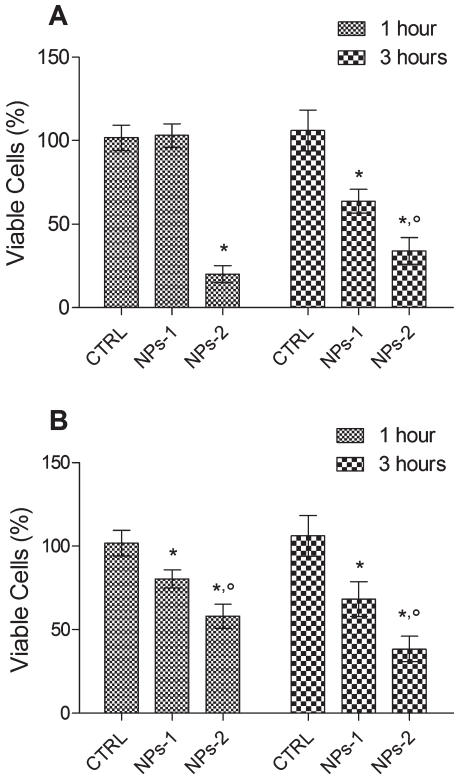

Figure 7. In vitro cytotoxicity of nontargeted (NPs-1) and targeted (NPs-2) nanoparticles on LNCaP cells pulsed for 1 and 3 h at a EGCG concentration of 30 μM after 48 h (A) and 72 h (B) incubation: (∗) significantly different from control; (○) significantly different from NP-1; $n = 3$.

NPs and following 48 h of exposure, there was not sufficient time to operate by a classical endocytosis mechanism. However, further investigation to explain this behavior is currently in progress.

In contrast, following 72 h of exposure to NPs-1 and NPs-2, similar antiproliferative profiles, with different inhibition values in the overall cell growth, were observed. In particular, with respect to control, 20% and ∼40% (for 1 h exposure) and ∼40% and 60% (for 3 h exposure) of growth inhibition values for NPs-1 and NPs-2, respectively, were calculated (Figure 7B). Also in this case, NPs-1 demonstrated lower efficacy with cells pulsed for 1 h than those evaluated from 3 h of exposure while enhanced potency was observed for NPs-2. By use of this experimental model, an improved antiproliferative activity for targeted PSMA with respect to the nontargeted EGCG loaded NPs was observed.

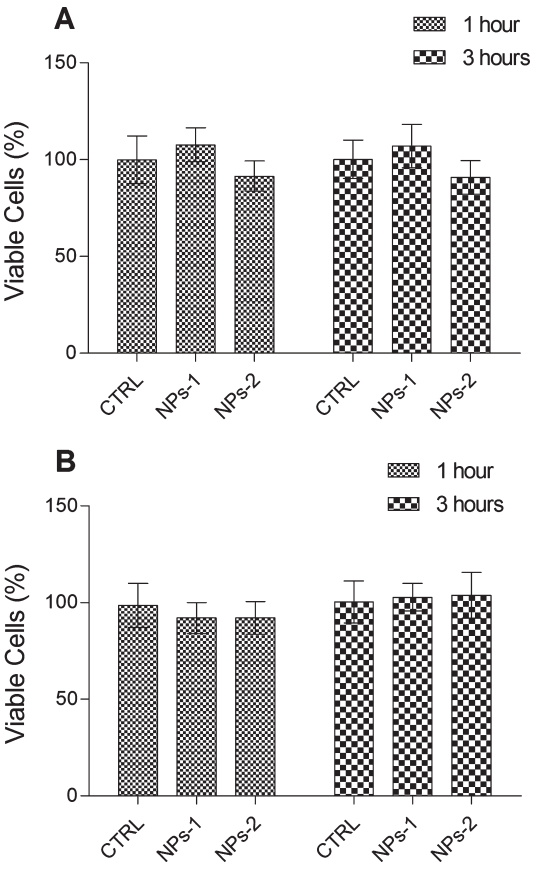

Figure 8. Inhibition of HUVECs proliferation by NPs-1 and NPs-2. Cells were pulsed for 1 and 3 h at a EGCG concentration of 30 μM after 48 h (A) and 72 h (B) of incubation.

To confirm that the difference in cytotoxicity is due to the DCL affinity to PSMA and to assess the selectivity of these prototypes against PCa cell lines, the in vitro inhibitory effects of NP-1 and NPs-2 on the proliferation of normal cells were also carried out. Thus, growth inhibition of HUVECs (human umbilical vein endothelial cells), as model system of normal cells, was measured by following the same protocol as described above. From the results shown in Figure 8, with about 100% cell survival, no significant cell growth suppression was observed for both nanosystems at a EGCG concentration of 30 μM after 48 and 72 h of exposure. These data suggest that EGCG-loaded NPs are equally ineffective in inhibiting HUVEC proliferation, whereas they selectively inhibit proliferation of PCa cells.

These results support the hypothesis that the primary role of target-specific ligands is to enhance cellular uptake of NPs and their load into cancer cells.

CONCLUSIONS

The fact that PCa onset and progression take considerable time to occur may be considered as an important opportunity for treating premalignant lesions. Therefore, since chemoprevention

by the use of EGCG proved to be an emerging approach for the treatment of early carcinogenic processes, we thought that the potent chemopreventive efficacy of this phytochemical for PCa could be improved by using targeted nanotechnology strategy. Moreover, this approach could also be exploited to enhance the bioavailability of EGCG by changing the pharmacokinetics and biodistribution.

In this work, we indirectly demonstrated that an EGCG-loaded NP system functionalized with a small organic molecule (PSMA inhibitor) on the surface significantly enhances binding to PSMA with respect to the nonfunctionalized ones, thus leading to an increased antiproliferative activity in in vitro assays toward PSMA-positive PCa cells, without affecting normal cell viability. From a comparison of EGCG encapsulated PSMA-targeted NPs to the nontargeted NPs, we demonstrated that the viability of LNCaP cells exposed to the PSMA-targeted particles was in general lower than the same particles without the targeting DCL. The cytotoxicity of EGCG loaded into the nontargeted NPs can be ascribed to a combination of nonspecific uptake and to the expected nonspecific release of EGCG into the medium over the exposure period. Meanwhile, the enhanced potency shared by EGCG encapsulated into targeted NPs can be attributed to the maximized binding between NPs and cells, which presumably would promote an active targeting to PSMA, resulting in enhanced accumulation and cell uptake through receptor (antigen) mediated endocytosis.

In summary, these results demonstrate that the effectiveness of EGCG encapsulated NPs, in terms of antiproliferative efficacy, can be significantly improved by incorporating specific ligands, such as small organic molecules, onto the NP surface in order to bind PSMA antigen present on PCa cells. The translational potential of these PSMA-targeted ECGC-loaded NPs warrants further in vivo studies in animal model. We expect that the insights obtained from this study can be useful to connect nanochemoprevention and targeting strategy toward management of PCa as a primary focus but also to be pursued as a validated model in a larger context.

EXPERIMENTAL SECTION

Materials. For preparation of NPs, poly(D,L-lactide-*co*-glycolide) (PLGA) (lactide/glycolide ratio of 50:50, inherent viscosity of 0.20 dL g^{-1} in hexafluoroisopropanol) with acid end groups were purchased from Lactel Absorbable Polymers (Pelham, AL, U.S.). The heterofunctional PEG polymer with a terminal amine and carboxylic acid functional group, NH_2-PEG-COOH (MW = 3400), was purchased from JenKem Technology USA. All solvents and other chemicals were obtained from Sigma-Aldrich, Carlo Erba, or ORPEGEN Peptide Chemicals GmbH. All reagents of commercial quality were used without further purification. Melting points (mp) were determined using an Electrothermal melting point or a Köfler apparatus and are uncorrected. Nuclear magnetic resonance (^{1}H NMR, ^{13}C NMR, ^{1}H−^{1}H COSY, ^{1}H−^{13}C HMBC, ^{1}H−^{13}C HSQC, and ^{1}H−^{1}H TOCSY) spectra were determined in $CDCl_3$, DMSO-d_6 or $CDCl_3$/DMSO-d_6 (in 3/1 ratio) and were recorded at 200, 500, and 600 MHz on a Varian XL-200, a Bruker Avance 500, and a Bruker AMX-600, respectively. Chemical shifts are reported in parts per million (ppm) downfield from tetramethylsilane (TMS), used as an internal standard. Splitting patterns are designated as follows: s, singlet; d, doublet; t, triplet; q, quadruplet; m, multiplet; brs, broad singlet; dd, double doublet. The assignment of exchangeable protons (O*H* and N*H*) was confirmed by the addition of D_2O. Electron ionization and MALDI TOF mass spectra (70 eV) were recorded on a Hewlett-Packard 5989 MS Engine spectrometer and by a MALDI micro MX (Waters, micromass) equipped with a reflectron analyzer. For MALDI TOF mass spectrometry (MS) analysis, the sample was mixed with an equal volume of matrix 2,5-dihydroxybenzoic acid (20 mg/mL in EtOH/H_2O (90:10, v/v), applied to the metallic sample plate, and air-dried. Mass calibration was carried out by using as a standard the antocyan mixture provided by the manufacturer. Analytical thin-layer chromatography (TLC) was carried out on Merck silica gel F-254 plates. Flash chromatography purifications were performed on Merck silica gel 60 (230−400 mesh ASTM) as a stationary phase. The purity of copolymers was determined by high performance liquid chromatography (HPLC) using an HP 1200 (Agilent Technologies, U.S.) system equipped with a Hypersil BDS C18 column (Alltech Italy, 250 mm × 4.6 mm i.d., 5 μm particle size); these materials were found to be >95% pure. Elemental analyses for **7** and DCL were performed on a Perkin-Elmer 2400 spectrometer at Laboratorio di Microanalisi, Dipartimento di Chimica, Università di Sassari (Italy), and were within ±0.4% of the theoretical values.

Molecular Modeling Studies. The X-ray crystal structure of the PSMA (GCPII) protein complexed with GPI-18431 inhibitor was retrieved from the Protein Data Bank (PDB code 2C6C)[39] and served as input structure for the docking studies. The ligands DCL and PEG-DCL were generated as follows: SMILES codes of the ligands were converted to a three-dimensional structure using the MOE program suite. The initial ligand structures were minimized, and the protonation states of amine and carboxy moieties were set properly. Rotatable bonds were kept flexible throughout the docking procedure.

For ligand docking, the genetic algorithm-based docking tool GOLD, version 4.0 (with GOLDscore), was employed. First, the target protein was loaded and protonated using the HERMES suite. Then 10 docking runs were performed for each ligand. For DCL, the following genetic algorithm parameters were employed: maximum number of operations = 85 000, population size = 100, selection pressure = 1.1, number of islands = 5, niche size = 2, cross weight = 95, mutation weight = 95, and migration weight = 10. For PEG-DCL, the same parameters were applied except for the maximum number of operations (150 000).

Synthesis of PLGA-PEG-COOH Block Copolymer. To a solution of PLGA-COOH (1.5 g, 0.083 mmol) in anhydrous methylene chloride (6 mL), *N*-hydroxysuccinimide (NHS, 38 mg, 0.33 mmol, 4 equiv) and 1-ethyl-3-(3-dimethylaminopropyl)carbodiimide (EDC, 70 mg, 0.36 mmol, 4.3 equiv) were added, and the reaction mixture was magnetically stirred at room temperature for 12 h under nitrogen atmosphere. PLGA-NHS was obtained by precipitation with cold diethyl ether (5 mL) as a white solid, which was filtered and repeatedly washed in a cold mixture of diethyl ether and methanol (few drops) to remove residual NHS, then dried with nitrogen and put under vacuum to remove solvent (yield, 97%). The intermediate PLGA-NHS (1.5 g, 0.085 mmol) was dissolved in anhydrous chloroform (5 mL). NH_2-PEG-COOH (0.375 g, 0.11 mmol, 1.3 equiv) and *N*,*N*-diisopropylethylamine (DIPEA) (42 mg, 0.325 mmol, 3.8 equiv) were then added under magnetic stirring. The reaction mixture was magnetically stirred at room temperature for 24 h. The desired copolymer was precipitated with cold diethyl ether and treated with the same solvents to remove unreacted PEG as described above (yield, 88%). The resulting PLGA-PEG block copolymer was dried under vacuum, characterized by ^{1}H NMR (200 and 600 MHz), and used for NP preparation without further treatment. ^{1}H NMR (500 MHz, $CDCl_3$) δ 5.23 (m, -OC-C*H*(CH_3)O-, PLGA), 4.78 (m, -OC-CH_2O-, PLGA), 3.65 (s, -CH_2CH_2O-, PEG), 1.56 (brs, -OC-CHCH_3O-, PLGA).

Synthesis of DCL and Intermediates. 2-{[(5-Amino-1-carboxypentyl)carbamoyl]amino}pentanedioic Acid (DCL). The intermediate (*S*)-2-[3-(5-amino-1-*tert*-butoxycarbonylpentyl)ureido]-pentanedioic acid di-*tert*-butyl ester **7** (130 mg, 0.17 mmol) was dissolved in 5 mL of 1:1 trifluoroacetic acid (TFA)/methylene chloride solution and stirred at room temperature for 3 h. Then the resulting solution was

evaporated under reduced pressure. The colorless solid residue was triturated with dry diethyl ether, filtered, and washed with dry diethyl ether to yield the desired product as an off beige solid (yield, 70%). ^{1}H NMR (600 MHz, DMSO-d_6) δ 7.80−7.60 (brs, 3H), 6.40−6.30 (s, 2H), 4.15−4.00 (m, 2H), 3.78−3.55 (m, 2H), 3.46−3.20 (brs, 1H), 2.78−2.72 (d, 2H), 2.27−2.22 (m, 2H), 2.00−1.85 (m, 2H), 1.76−1.59 (m, 2H), 1.53−1.47 (m, 2H), 1.38−1.19 (m, 2H). MS (MALDI-TOF): [M^+ 319]; [M^+ 319 + Na, 342]. EI: [M^+ 319]. Anal. ($C_{12}H_{21}N_3O_7\cdot$ 1.15CF_3COOH) C, H, N.

Preparation of 2-{3-[1-*p*-Methoxybenzylcarboxylate (5-*tert*-Butylcarbamylpentyl)]ureido}-di-*p*-methoxybenzyl-pentanedioate (7). Triphosgene (0.18 g, 0.613 mmol) was placed in a flame-dried flask cooled to 0 °C, under nitrogen atmosphere, and a solution of **3** (0.68 g, 1.86 mmol, 3 equiv) and TEA (0.53 mL, 3.72 mmol, 6 equiv) dissolved in CH_2Cl_2 (3 mL) was added. The reaction mixture was stirred at 0 °C for 15 min. A mixture of **6** (0.79 g, 1.86 mmol, 3 equiv) and TEA (0.53 mL, 3.72 mmol, 6 equiv) in CH_2Cl_2 (3 mL) was then added. The resulting mixture was allowed to warm to room temperature and stirred for 2 h. Product was extracted by CH_2Cl_2, washed with water and brine, and dried over Na_2SO_4. Purification by flash chromatography (20/80 EtOAc/CH_2Cl_2) afforded an oil that solidified upon standing (yield, 59%). ^{1}H NMR ($CDCl_3$) δ 7.26 (d, 6H), 6.87 (d, 6H), 5.52 (d, 2H), 5.13−4.98 (m, 6H), 4.76 (brs, 1H), 4.53−4.48 (m, 1H), 4.50−4.43 (m, 1H), 3.79 (s, 9H), 3.04−2.96 (m, 2H), 2.40−2.34 (m, 2H), 2.14−2.11 (m, 2H), 1.94−1.70 (m, 2H), 1.60−1.56 (m, 2H), 1.42 (s, 9H), 1.25−1.22 (m, 2H). MS-ESI: 780 [$M + 1$]$^+$. Anal. ($C_{41}H_{53}N_3O_{12}$) C, H, N.

Preparation of 2-Amino-6-*tert*-butoxycarbonylamino-hexanoic Acid 4-Methoxybenzyl Ester (3). To a solution of *N*ε-Boc-*N*-Fmoc-L-lysine (**1**, 8.16 g, 17.41 mmol) in 70 mL of dry DMF, cesium carbonate (8.14 g, 24.4 mmol, 1.4 equiv) and 4-methoxybenzyl chloride (PMBC, 3.0 g, 2.6 mL, 19.15 mmol, 1.1 equiv) were added under nitrogen atmosphere, and the suspension was stirred at room temperature for 4 h. The reaction mixture was then filtered, sequentially washed with ethyl acetate, 5% Na_2CO_3, water, and dried over Na_2SO_4. Purification by recrystallization from 60/40 hexane/EtOAc gave a beige powder corresponding to compound **2** (yield, 95%). Mp 117−119 °C (lit. 118−120 °C).[45] ^{1}H NMR($CDCl_3$) δ 8.12 (s, 1H), 7.76−7.67 (m, 4H), 7.40−7.25 (m, 6H), 6.89 (d, 2H), 5.29 (s, 1H), 5.08 (s, 2H), 4.53−4.42 (m, 1H), 4.09 (t, 2H), 3.80 (s, 3H), 3.07−2.98 (m, 3H), 1.92−1.10 (m, 15H). MS-ESI m/z: 588 [$M + 1$]$^+$. A solution of compound **2** (8.44 g, 14.4 mmol) in 100 mL of a 20% solution of piperidine in DMF was stirred at room temperature for 2 h. Product was extracted by CH_2Cl_2, washed with water, and dried over Na_2SO_4. The crude residue was purified by silica gel flash chromatography (5/95 MeOH/CH_2Cl_2, 20/80 EtOAc/CH_2Cl_2, 10/90 EtOAc/CH_2Cl_2). Compound **3** was obtained as a yellow oil (yield, 71%). ^{1}H NMR ($CDCl_3$) δ: 8.02 (brs, 2H), 7.30 (d, 2H), 6.89 (d, 2H), 5.30 (s, 1H), 5.09 (s, 2H), 4.58−4.40 (m, 1H), 3.83 (s, 3H), 3.08−2.28 (m, 2H), 2.05−1.18 (m, 15H). MS-ESI m/z: 367 [$M + 1$]$^+$.

Bis-4-methoxybenzylglutamate Hydrochloride (6). To an ice-cooled mixture of amino acid **4** (8.0 g, 54.4 mmol) in dry DMF (10 mL), *N*,*N*,*N*′,*N*′-tetramethylguanidine (13.4 mL, 108.8 mmol, 2 equiv) was added. After 30 min under magnetic stirring, ethyl acetoacetate (13.84 mL, 108.8 mmol, 2 equiv) was added and stirring was continued at room temperature until the amino acid had dissolved. PMBC (16.98 g, 7.36 mL, 108.8 mmol, 2 equiv) in DMF (55 mL) was added, and stirring continued at room temperature for 24 h. The reaction mixture was then diluted with ethyl acetate, washed with water, 1 N $NaHCO_3$, and dried over Na_2SO_4 to afford compound **5** as a yellow oil. ^{1}H NMR ($CDCl_3$) δ 8.80−8.72 (d, 2H), 7.27 (d, 4H), 6.87 (d, 4H), 5.10 (s, 2H), 5.03 (s, 2H), 4.24−4.15 (m, 1H), 3.80 (s, 6H), 2.45−2.38 (m, 2H), 2.28−2.00 (m, 2H). The product (compound **5**) was treated with hydrogen chloride 4 N solution in diethyl ether to give chlorohydrate **6** as a white powder (yield, 84%). Mp 114−116 °C (lit. 114−115 °C).[50] ^{1}H NMR ($CDCl_3$) δ 8.89 (brs, 3H), 7.20 (d, 4H), 6.81 (d, 4H), 5.08 (brs, 2H), 4.94 (s, 2H), 4.41−4.23 (m, 1H), 3.76 (s, 3H), 3.74 (s, 3H), 2.72−2.50 (m, 2H), 2.49−2.31 (m, 2H).

Preparation of (2*S*,2′*S*)-1,5-Bis(4-methoxybenzyl)-2,2′-carbonylbis(azanediyl)dipentanedioate (8). To a mixture of bis-4-methoxybenzyl-L-glutamate·HCl **6** (3.6 g, 8.5 mmol, 3 equiv) in 15 mL of CH_2Cl_2, a solution of triphosgene (0.833 g, 2.8 mmol) dissolved in 3 mL of CH_2Cl_2 was added under nitrogen atmosphere. After the mixture was cooled to −78 °C, TEA (12 mL, 85 mmol in 10 mL of CH_2Cl_2, 30 equiv) was slowly added. The reaction mixture was stirred at −78 °C for 1 h, allowed to warm at room temperature, and stirred for a further 30 min at room temperature. Compound **3** (3.1 g, 8.5 mmol in 7 mL CH_2Cl_2, 3 equiv) was then added, and the resulting mixture was continually stirred overnight. Product was extracted by CH_2Cl_2, washed with water and brine, and dried over Na_2SO_4. Purification by flash chromatography (20/80 EtOAc/CH_2Cl_2) afforded an oil that solidified upon standing (yield, 62%). Mp 97−99 °C. ^{1}H NMR ($CDCl_3$) δ 7.25 (d, 8H), 6.85 (d, 8H), 5.29 (s, 1H), 5.25 (s, 1H), 5.05 (s, 4H), 5.01 (s, 4H), 4.52−4.46 (m, 2H), 3.79 (s, 12H), 2.41−2.22 (m, 4H), 2.20−1.78 (m, 4H). MS-ESI m/z: 801 [$M + 1$]$^+$.

Synthesis of PLGA-PEG-DCL Pseudo-Tri-Block-Copolymer. To a solution of PLGA-PEG-COOH di-block-copolymer (1.4 g, 0.065 mmol) in anhydrous methylene chloride (5 mL), NHS (30 mg, 0.26 mmol, 4 equiv) and EDC (53 mg, 0.28 mmol, 4.3 equiv) were added, and the solution was magnetically stirred at room temperature for 12 h under nitrogen atmosphere. The activated PLGA-PEG-NHS copolymer was precipitated in ice-cold diethyl ether and methanol (few drops), consequently filtered and dried, as described above, to give a white powder (yield, 92%). The PLGA-PEG-DCL was obtained by the addition of a solution of DCL salt (38 mg, 0.088 mmol, 4 equiv) in DMF (1 mL) and DIPEA (0.72 mL, 0.0041 mol) to a solution of PLGA-PEG-NHS (0.45 g, 0.022 mmol) in dimethylformamide (DMF, 2.5 mL), and the reaction mixture was magnetically stirred at room temperature for 24 h under nitrogen atmosphere. PLGA-PEG-DCL was analyzed by high performance liquid chromatography (HPLC) on a Hypersil BDS C18 column (Alltech Italy), (250 mm × 4.6 mm i.d., 5 μm particle size), using as eluent a linear gradient of eluent B (95% MeCN, 0.07% TFA) in A (0.1% TFA) from 15% to 100% for 30 min (flow rate of 1 mL/min, temperature at 25 °C, and a detector wavelength of 280 nm). The equipment consisted of an HP 1200 (Agilent Technologies, U.S.) system controlled by HP ChemStation software, including an autosampler and a diode array detector. After purification, a white solid was obtained (yield, 65%), which was characterized by ^{1}H NMR and UV analysis. The polymer was then freeze-dried and stored at −20 °C before use.

Formulation and Characterization of EGCG-Loaded PLGA-PEG-COOH and PLGA-PEG-DCL NPs. *Preparation of EGCG-Loaded NPs.* NPs were prepared by modification of nanoprecipitation method.[44] Briefly, polymer (PLGA-PEG or PLGA-PEG-DCL) (100 mg) and EGCG (5 mg) were co-dissolved in acetonitrile (10 mL) and added dropwise into 7.5 mL of water. The milky colloidal suspension was evaporated at room temperature to eliminate residual organic solvent. NPs were isolated by centrifugation (10 min, 14 000 rpm) and washed three times with water to remove the nonencapsulated EGCG. The pellets were suspended in 1.5 mL of water and stored at 4 °C until use. A part of the nanoparticle aqueous dispersion was rapidly frozen below −80 °C in a deep-freezer, lyophilized (5 Pascal LIO 5P apparatus, Cinquepascal SRL, Milano, Italy), and collected for other experiments.

Scanning Electron Microscopy (SEM). The morphology (shape and surface characteristics) of NPs was studied by scanning electron microscopy (SEM) (model DSM 962, Carl Zeiss Inc., Germany). A drop of NP suspension was placed on a glass cover slide and dried under vacuum

for 12 h. After that, the slides were mounted on an aluminum stub and the samples were then analyzed at 25 kV acceleration voltage after gold sputtering under an argon atmosphere. The size of NPs was determined by measuring more than 100 particles from SEM images.

Determination of EGCG Content in NPs and Yields of Production. The amount of the encapsulated EGCG was determined by dissolving a weighted amount (10 mg) of dried EGCG loaded NPs in methylene chloride (1 mL) and measured using a validated HPLC method.[51] The EGCG content was expressed as μg/mg of the NPs mass and the encapsulation efficiency calculated as a percentage ratio of measured and initial amount of EGCG encapsulated into NPs. Chromatographic analysis was performed on a HP 1200 (Agilent Technologies, U.S.) liquid chromatography system equipped with a diode array detector of the same series, using a Jupiter C18 (5 μm pore size) 250 mm × 2.0 mm column (Phenomenex). The mobile phase consisting of water/acetonitrile/methanol/ethyl acetate/glacial acetic acid (89:6:1:3:1 v/v/v/v/v) was prepared daily and degassed by sonication for 30 min and filtered through a φ 55 mm blue ribbon filter paper before use. The column was thermostated at 20 °C. The method[51] was modified and delivered isocratically with a flow rate of 0.2 mL/min. The injection volume was 25 μL, and the wavelength for UV detection was 280 nm. The total analysis time was 30 min, and the retention time of EGCG was 12.86 min. The calibration curves were found to be linear in the range of 5−50 μg/mL ($y = 925.38x + 42.047$; $R^2 = 0.9999$). The yields of production were expressed as the weight percentage of the final product after drying, regarding the initial total amount of solid materials used for the preparation.

In Vitro Release Kinetics of EGCG from NPs. The in vitro release profile of EGCG from NPs was assessed by the determination of the residual amount of EGCG present in the NPs. The tests were performed in water (pH 6.4) at room temperature and in phosphate buffer solution (PBS) with different pH (pH 6.7 and pH 7.4) at 37 °C. For that purpose, several aliquots (100 μL) of the original suspensions of NPs were diluted with release medium (final volume of 1 mL) in a 1.5 mL vial and continuously shaken at the selected temperature. At predetermined time intervals, the sample vial was centrifuged at 14 000 rpm for 5 min, and the precipitate was washed twice with distilled water and lyophilized. The dried sample was then dissolved in 100 μL of methylene chloride and analyzed by HPLC using the previously described procedure. Every 30 min, all sample vials were centrifuged, the pellet was washed once with water, and the supernatant was replaced with fresh medium for the next release data collection. The percentage of EGCG release at a specific timing was calculated on the basis of the total amount measured from sample NPs. The dissolution of EGCG as raw material was made in the same conditions as comparison. Each sample was assayed in triplicate. To study NP−EGCG interaction, 30 μL of PLGA-PEG-COOH-based unloaded NPs (1.34 mg) and 8 μL (1 mg/mL) of EGCG in 142 μL of water were mixed and stirred at room temperature. Samples were analyzed by HPLC (after 0.5, 1, 2, 5, 10 h) with a diode array detector using the same procedure previously described.

In Vitro Cytotoxicity Assays to PSMA Expressing PCa Cells (LNCaP) and Human Umbilical Veins Endothelial Cells (HUVEC). LNCaP cell lines (ECACC, Salisbury, U.K.) were grown in 24-well plates with RPMI 1640 medium containing 100 units/mL penicillin G, 100 μg/mL streptomycin, and 10% FBS (Invitrogen, Carlsbad, CA) at a concentration that allows 70% confluence in 48 h. HUVECs (Cell Applications, San Diego, CA) were cultured in endothelial cell basal medium (Cell Applications) supplemented with endothelial cell growth supplement (Cell Applications). When confluent, HUVECs were subcultured at a split ratio of 1:2 and used within three passages. For proliferation experiments, cells were transferred to 24-well plates at a concentration that allows 70% confluence in 48 h. On the day of the experiments, similar treatment was applied for both cell types. Cells were washed with PBS and then exposed for 1 or 3 h with 100 μL of a suspension of EGCG loaded NPs (NP-1 or NPs-2) in serum-free culture medium to a final concentration of 30 μM EGCG. Cells were washed three times with PBS (100 μL), and fresh growth medium was replaced in the plates. Cells were then incubated in medium at 37 °C, and at the end of 48 and 72 h, effects on cell growth were determined by automatic cell counting (Countess Invitrogen) and expressed as percent of the number of cells per mL.

Statistical Analysis. The data for preparation and characterization of NPs as well as drug release studies were processed and analyzed by Origin software (version 7.0 SR0, OriginLab Corporation, U.S.). The statistical analysis was evaluated by a Student's *t*-test, and $p < 0.05$ was considered statistically significant. The data obtained from cytotoxicity assays were processed by one-way analysis of variance (ANOVA) followed by a post hoc "Newman−Keuls multiple comparison test" to detect differences of mean values among treatments with significance defined as $p < 0.05$.

AUTHOR INFORMATION

Corresponding Author

*For M.S.: phone, +39 079-228-753; fax, +39 079-228-720; e-mail, mario.sechi@uniss.it. For V.S.: phone, +39 079-998-619; fax, +39 079-228-720; e-mail, sannav@portocontericerche.it. For G.P.: phone, +39 079-228-121; fax, +39 079-228-120; e-mail, gpintus@uniss.it.

Notes

⊥The department name was changed on January 31, 2011. Current address is Dipartimento di Scienze del Farmaco, Università di Sassari, 07100 Sassari, Italy.

ACKNOWLEDGMENT

The research activities presented were done within the frame of "Progetto Cluster, Sviluppo ed Utilizzo di Nanodevices", funded by Sardinian Technology Park, Porto Conte Ricerche, Italy. The authors thank Dr. Roberto Anedda, Dr. Maria Orecchioni, and Paolo Fiori for assistance with NMR spectroscopy. The authors also thank Dr. Martin Sippel, Dr. Monika Nocker, and Dr. Nicolino Pala for their generous contribution of the time spent on the elaboration of the molecular modeling calculation and images.

ABBREVIATIONS USED

NPs, nanoparticles; PLGA, poly-(D,L-lactide-*co*-glicolyde); PLGA-PEG, poly(D,L-lactic-*co*-glycolic acid)-*block*-poly(ethylene glycol); DCL, *N*-[*N*-[(*S*)-1,3-dicarboxypropyl]carbamoyl]-(*S*)-lysine; GTCs, green tea catechin; EGCG, (−)-epigallocatechin 3-gallate; PSMA, prostate-specific membrane antigen; PCa, prostate cancer; HG-PIN, high-grade prostatic intraepithelial neoplasia; GCPII, glutamate carboxypeptidase; HUVECs, human umbilical vein endothelial cells

REFERENCES

(1) Farokhzad, O. C.; Langer, R. Impact of nanotechnology on drug delivery. *ACS Nano* **2009**, *3*, 16–20.

(2) Peer, D.; Karp, J. M.; Hong, S.; Farokhzad, O. C.; Margalit, R.; Langer, R. Nanocarriers as an emerging platform for cancer therapy. *Nat. Nanotechnol.* **2007**, *2*, 751–760.

(3) Ferrari, M. Cancer nanotechnology: opportunities and challenges. *Nat. Rev. Cancer* **2005**, *5*, 161–171.

(4) Davis, M. E.; Chen, Z. G.; Shin, D. M. Nanoparticle therapeutics: an emerging treatment modality for cancer. *Nat. Rev. Cancer* **2008**, *7*, 771–782.

(5) Zhang, L.; Gu, F. X.; Chan, J. M.; Wang, A. Z.; Langer, R. S.; Farokhzad, O. C. Nanoparticles in medicine: therapeutic applications and developments. *Clin. Pharmacol. Ther.* **2008**, *83*, 761–769.

(6) Shi, J.; Votruba, A. R.; Farokhzad, O. C.; Langer, R. Nanotechnology in drug delivery and tissue engineering: from discovery to applications. *Nano Lett.* **2010**, *10*, 3223–3230.

(7) Gu, F.; Langer, R.; Farokhzad, O. C. Formulation/preparation of functionalized nanoparticles for in vivo targeted drug delivery. *Methods Mol. Biol.* **2009**, *544*, 589–598.

(8) Byrne, J. D.; Betancourt, T.; Brannon-Peppas, L. Active targeting schemes for nanoparticle systems in cancer therapeutics. *Adv. Drug Delivery Rev.* **2008**, *60*, 1615–1626.

(9) Alexis, F.; Pridgen, E.; Molnar, L. K.; Farokhzad, O. C. Factors affecting the clearance and biodistribution of polymeric nanoparticles. *Mol. Pharmaceutics* **2008**, *5*, 505–515.

(10) Alexis, F.; Pridgen, E. M.; Langer, R.; Farokhzad, O. C. Nanoparticle technologies for cancer therapy. *Handb. Exp. Pharmacol.* **2010**, *197*, 55–86.

(11) Siu, D. Cancer therapy using tumor-associated antigens to reduce side effects. *Clin. Exp. Med.* **2009**, *9*, 181–198.

(12) Cozzi, P. J.; Kearsley, J.; Li, Y. Overview of tumor-associated antigens (TAAs) as potential therapeutic targets for prostate cancer therapy. *Curr. Cancer Ther. Rev.* **2008**, *4*, 271–284.

(13) Chang, S. S.; O'Keefe, D. S.; Bacich, D. J.; Reuter, V. E.; Heston, W. D.; Gaudin, P. B. Prostate-specific membrane antigen is produced in tumor-associated neovasculature. *Clin. Cancer Res.* **1999**, *5*, 2674–2681.

(14) Ghosh, A.; Heston, W. D. Tumor target prostate specific membrane antigen (PSMA) and its regulation in prostate cancer. *J. Cell. Biochem.* **2004**, *91*, 528–539.

(15) Schülke, N.; Varlamova, O. A.; Donovan, G. P.; Ma, D.; Gardner, J. P.; Morrissey, D. M.; Arrigale, R. R.; Zhan, C.; Chodera, A. J.; Surowitz, K. G.; et al. The homodimer of prostate-specific membrane antigen is a functional target for cancer therapy. *Proc. Natl. Acad. Sci. U.S.A.* **2003**, *100*, 12590–12595.

(16) Elsässer-Beile, U.; Bühler, P.; Wolf, P. Targeted therapies for prostate cancer against the prostate specific membrane antigen. *Curr. Drug Targets* **2009**, *10*, 118–125.

(17) Farokhzad, O. C.; Cheng, J.; Teply, B. A.; Sherifi, I.; Jon, S.; Kantoff, P. W.; Richie, J. P.; Langer, R. Targeted nanoparticle−aptamer bioconjugates for cancer chemotherapy in vivo. *Proc. Natl. Acad. Sci. U.S. A.* **2006**, *103*, 6315–6320.

(18) Gu, F.; Zhang, L.; Teply, B. A.; Mann, N.; Wang, A.; Radovic-Moreno, A. F.; Langer, R.; Farokhzad, O. C. Precise engineering of targeted nanoparticles by using self-assembled biointegrated block copolymers. *Proc. Natl. Acad. Sci. U.S.A.* **2008**, *105*, 2586–2591.

(19) Surh, Y.-J. Cancer chemoprevention with dietary phytochemicals. *Nat. Rev. Cancer* **2003**, *3*, 768–780.

(20) Siddiqui, I. A.; Mukhtar, H. Nanochemoprevention by bioactive food components: a perspective. *Pharm. Res.* **2010**, *27*, 1054–1060.

(21) Siddiqui, I. A.; Adhami, V. M.; Ahmad, N.; Mukhtar, H. Nanochemoprevention: sustained release of bioactive food components for cancer prevention. *Nutr. Cancer* **2010**, *62*, 883–890.

(22) Saleem, M.; Adhami, V. M.; Siddiqui, I. A.; Mukhtar, H. Tea beverage in chemoprevention of prostate cancer: a mini-review. *Nutr. Cancer* **2003**, *47*, 13–23.

(23) Yang, C. S.; Wang, X.; Lu, G.; Picinich, S. C. Cancer prevention by tea: animal studies, molecular mechanisms and human relevance. *Nat. Rev. Cancer* **2009**, *9*, 429–439.

(24) Johnson, J. J.; Bailey, H. H.; Mukhtar, H. Green tea polyphenols for prostate cancer chemoprevention: a translational perspective. *Phytomedicine* **2010**, *17*, 3–13.

(25) Khan, N.; Adhami, V. M.; Mukhtar, H. Review: green tea polyphenols in chemoprevention of prostate cancer: preclinical and clinical studies. *Nutr. Cancer* **2009**, *61*, 836–841.

(26) Kurahashi, N.; Sasazuki, S.; Iwasaki, M.; Inoue, M.; Tsugane, S. Green tea consumption and prostate cancer risk in Japanese Men: a prospective study. *Am. J. Epidemiol.* **2008**, *167*, 71–77.

(27) Siddiqui, I. A.; Adhami, V. M.; Bharali, D. J.; Hafeez, B. B.; Asim, M.; Khwaja, S. I.; Ahmad, N.; Cui, H.; Mousa, S. A.; Mukhtar, H. Introducing nanochemoprevention as a novel approach for cancer control: proof of principle with green tea polyphenol epigallocatechin-3-gallate. *Cancer Res.* **2009**, *69*, 1712–1716.

(28) Bettuzzi, S.; Brausi, M.; Rizzi, F.; Castagnetti, G.; Peracchia, G.; Corti, A. Chemoprevention of human prostate cancer by oral administration of green tea catechins in volunteers with high-grade prostate intraepithelial neoplasia: a preliminary report from a one-year proof-of-principle study. *Cancer Res.* **2006**, *66*, 1234–1240.

(29) Brausi, M.; Rizzi, F.; Bettuzzi, S. Chemoprevention of human prostate cancer by green tea catechins: two years later. A follow-up update. *Eur. Urol.* **2008**, *54*, 472–473.

(30) Leonarduzzi, G.; Testa, G.; Sottero, B.; Gamba, P.; Poli, G. Design and development of nanovehicle-based delivery systems for preventive or therapeutic supplementation with flavonoids. *Curr. Med. Chem.* **2010**, *17*, 74–95.

(31) Otsuka, H.; Nagasaki, Y.; Kataoka, K. PEGylated nanoparticles for biological and pharmaceutical applications. *Adv. Drug Delivery Rev.* **2003**, *55*, 403–419.

(32) Avgoustakis, K. Pegylated poly(lactide) and poly(lactide-coglycolide) nanoparticles: preparation, properties and possible applications in drug delivery. *Curr. Drug Delivery* **2004**, *1*, 321–333.

(33) Betancourt, T.; Byrne, J. D.; Sunaryo, N.; Crowder, S. W.; Kadapakkam, M.; Patel, S.; Casciato, S.; Brannon-Peppas, L. PEGylation strategies for active targeting of PLA/PLGA nanoparticles. *J. Biomed. Mater. Res., Part A* **2009**, *91*, 263–276.

(34) Chandran, S. S.; Banerjee, S. R.; Mease, R. C.; Pomper, M. G.; Denmeade, S. R. Characterization of a targeted nanoparticle functionalized with a urea-based inhibitor of prostate-specific membrane antigen (PSMA). *Cancer Biol. Ther.* **2008**, *7*, 974–982.

(35) Maresca, K. P.; Hillier, S. M.; Femia, F. J.; Keith, D.; Barone, C.; Joyal, J. L.; Zimmerman, C. N.; Kozikowski, A. P.; Barrett, J. A.; Eckelman, W. C.; et al. A series of halogenated heterodimeric inhibitors of prostate specific membrane antigen (PSMA) as radiolabeled probes for targeting prostate cancer. *J. Med. Chem.* **2009**, *52*, 347–357.

(36) Byun, Y.; Mease, R. C.; Lupold, S. E.; Pomper, M. G. In *Drug Design of Zinc−Enzyme Inhibitors: Functional, Structural, and Disease Applications*; Supuran, C. T., Winum, J.-Y., Eds.; Binghe Wang Wiley Series in Drug Discovery and Development; John Wiley and Sons: Hoboken, NJ, 2009; pp 881−910.

(37) Zhou, J.; Neale, J. H.; Pomper, M. G.; Kozikowski, A. P. NAAG peptidase inhibitors and their potential for diagnosis and therapy. *Nat. Rev. Drug Discovery* **2005**, *4*, 1015–1026.

(38) Davis, M. I.; Bennett, M. J.; Thomas, L. M.; Bjorkman, P. J. Crystal structure of prostate-specific membrane antigen, a tumor marker and peptidase. *Proc. Natl. Acad. Sci. U.S.A.* **2005**, *102*, 5981–5986.

(39) Mesters, J. R.; Barinka, C.; Li, W.; Tsukamoto, T.; Majer, P.; Slusher, B. S.; Konvalinka, J.; Hilgenfeld, R. Structure of glutamate carboxypeptidase II, a drug target in neuronal damage and prostate cancer. *EMBO J.* **2006**, *25*, 1375–1384.

(40) Barinka, C.; Byun, Y.; Dusich, C. L.; Banerjee, S. R.; Chen, Y.; Castanares, M.; Kozikowski, A. P.; Mease, R. C.; Pomper, M. G.; Lubkowski, J. Interactions between human glutamate carboxypeptidase II and urea-based inhibitors: structural characterization. *J. Med. Chem.* **2008**, *51*, 7737–7743.

(41) Barinka, C.; Rovenská, M.; MLcochová, P.; Hlouchová, K.; Plechanovová, A.; Majer, P.; Tsukamoto, T.; Slusher, B. S.; Konvalinka, J.; Lubkowski, J. Structural insight into the pharmacophore pocket of human glutamate carboxypeptidase II. *J. Med. Chem.* **2007**, *50*, 3267–3273.

(42) Gref, R.; Minamitake, Y.; Peracchia, M. T.; Trubetskoy, V.; Torchilin, V.; Langer, R. Biodegradable long-circulating polymeric nanospheres. *Science* **1994**, *263*, 1600–1603.

(43) Gref, R.; Luck, M.; Quellec, P.; Marchand, M.; Dellacherie, E.; Harnisch, S.; Blunk, T.; Muller, R. H. "Stealth" corona-core nanoparticles surface modified by polyethylene glycol (PEG): influences of the corona (PEG chain length and surface density) and of the core

composition on phagocytic uptake and plasma protein adsorption. *Colloids Surf., B* **2000**, *18*, 301–313.

(44) Cheng, J.; Teply, B. A.; Sherifi, I.; Sung, J.; Luther, G.; Gu, F. X.; Levy-Nissenbaum, E.; Radovic-Moreno, A. F.; Langer, R.; Farokhzad, O. C. Formulation of functionalized PLGA-PEG nanoparticles for in vivo targeted drug delivery. *Biomaterials* **2007**, *28*, 869–876.

(45) Banerjee, S. R.; Foss, A. C.; Castanares, M.; Mease, R. C.; Byun, Y.; Fox, J. J.; Hilton, J.; Lupold, S. E.; Kozikowski, A. P.; Pomper, M. G. Synthesis and evaluation of technetium-99m- and rhenium-labeled inhibitors of the prostate-specific membrane antigen (PSMA). *J. Med. Chem.* **2008**, *51*, 4504–4517.

(46) Maclaren, J. A. Some amino acid esters—an improved preparative method. *Aust. J. Chem.* **1978**, *31*, 1865–1868.

(47) Lee, E. S.; Oh, K. T.; Kim, D.; Youn, Y. S.; Bae, Y. H. Tumor pH-responsive flower-like micelles of poly(L-lactic acid)-*b*-poly(ethylene glycol)-*b*-poly(L-histidine). *J. Controlled Release* **2007**, *123*, 19–26.

(48) Shutava, T. G.; Balkundi, S. S.; Vangala, P.; Steffan, J. J.; Bigelow, R. L.; Cardelli, J. A.; O'Neal, D. P.; Lvov, Y. M. Layer-by-layer-coated gelatin nanoparticles as a vehicle for delivery of natural polyphenols. *ACS Nano* **2009**, *3*, 1877–1885.

(49) Hu, B.; Pan, C.; Sun, Y.; Hou, Z.; Ye, Y.; Hu, B.; Zeng, X. Optimization of fabrication parameters to produce chitosan-tripolyphosphate nanoparticles for delivery of tea catechins. *J. Agric. Food Chem.* **2008**, *56*, 7451–7458.

(50) Mease, R. C.; Dusich, C. L.; Foss, C. A.; Ravert, H. T.; Dannals, R. F.; Seidel, J.; Prideaux, A.; Fox, J. J.; Sgouros, G.; Kozikowski, A. P.; Pomper, M. G. *N*-[*N*-[(*S*)-1,3-Dicarboxypropyl]carbamoyl]-4-[^{18}F]fluorobenzyl-L-cysteine, [^{18}F]DCFBC: a new imaging probe for prostate cancer. *Clin. Cancer Res.* **2008**, *14*, 3036–3043.

(51) Saito, S. T.; Welzel, A.; Suyenaga, E. S.; Bueno, F. A method for fast determination of epigallocatechin gallate (EGCG), epicatechin (EC), catechin (C) and caffeine (CAF) in green tea using HPLC. *Cienc. Tecnol. Aliment.* **2006**, *26*, 394–400.